Enhanced performance of hydroxyl and cyano groups functionalized graphitic carbon nitride for efficient removal of crystal violet and methylene blue from wastewater

Nada M. Ghazy[1], Eslam A Ghaith[1], Y.G. Abou El-Reash[1,2], Rania R. Zaky[1], Weam M. Abou El-Maaty[1], and Fathi S. Awad[1,*]

[1]Chemistry Department, Faculty of Science, Mansoura University, Mansoura 35516, Egypt. E-mail: fathyawad949@yahoo.com; fathysamy@mans.edu.eg
[2] Chemistry Department, Faculty of Science, Imam Mohammad Ibn Saud Islamic University, P.O. Box, 90950, Riyadh 11623, Saudi Arabia.

Supporting Information

S1. Materials. High purity 99.5%, 2.4,6-triazine and anhydrous potassium hydroxide (KOH, 99.95%) were provided by Sigma-Aldrich. Methylene blue (MB) and crystal violet (CV) were acquired from Thermo Fisher Co. (USA). All solutions were prepared using distilled water and all components were used without further purification.

S2. Characterization. The pristine g-C_3N_4 and F/g-C_3N_4 were characterized by x-ray Photoelectron Spectroscopy (XPS) using the Termo Fisher ESCAlab 250, FT-IR spectroscopy using the Nicolet-Nexus 670 FTIR spectrometer (4 cm-1 resolution and 32 scan), X-ray diffraction using an X'Pert Philips Materials Research Diffractometer, and SEM with a Hitachi SU-70 FE-SEM.

S3.

The PFO model usually predicts the behavior at the initial stage of the adsorption process, while PSO model predicts the behavior at all stages of the adsorption process[1].

Pseudo-first-order kinetic model:

$$\log\left(q_e - q_t\right) = \log q_e - \frac{K_1 t}{2.303} \qquad (3)$$

Pseudo-second-order kinetic model:

$$\frac{t}{q_t} = \frac{1}{K_2 {q_e}^2} + \frac{t}{q_e} \qquad (4)$$

Where k_1 (min^{-1}) and k_2 (g mol^{-1} min^{-1}) are the rate constants. q_t and q_e are the adsorption uptake of heavy metal at time t (min) and at equilibrium. Where k_1 (min^{-1}) and k_2 (g mol^{-1} min^{-1}) are the rate constants. q_t and q_e are the adsorption uptake of heavy metal at time t (min) and at equilibrium.

S4.

The Langmuir and Freundlich isotherm models are two extensively used mathematical models. The Langmuir model assumes a monolayer coverage and that all the adsorbent sorption sites are the same while the Freundlich isotherm model assumes that the coverage is multilayer and that all the adsorption sites are heterogenous. The Langmuir and Freundlich models are presented as Eq.(1) and Eq. [2], respectively, as follows:[2-3]

$$\ln q_e = lnK_f + \frac{1}{n} lnC_e \qquad (1)$$

$$\frac{C_e}{q_e} = \frac{1}{b\,Q_0} + \frac{C_e}{Q_0} \qquad (2)$$

Where q_e, C_e, b, and Q_o are the equilibrium adsorption capacity, the equilibrium concentration of the metal ions, the Langmuir constant, and the Langmuir monolayer adsorption capacity, respectively. 1/n and K_f are the adsorption intensity and the Freundlich constant, respectively.

Moreover, the essential feature of the Langmuir isotherm can be defined as RL parameter given by **Eq. (5)**.[4]

$$R_L = \frac{1}{1 + bc_0} \qquad (5)$$

The separation factor (R_L) can be used to indicate the shape of the adsorption behavior to be either irreversible ($R_L = 0$), linear ($R_L = 1$), unfavorable ($R_L > 1$), or favorable ($0 < R_L < 1$).[5]

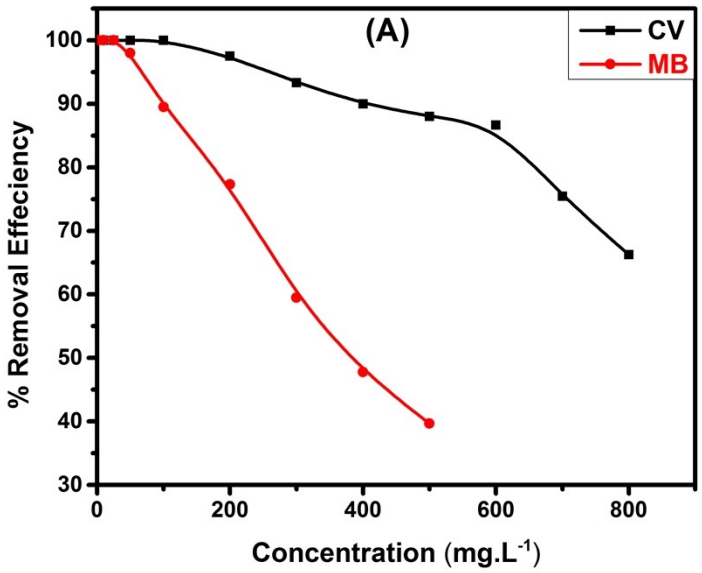

Figure S1: Dependence of the removal efficiency of CV and MB onto f/g-CN on the initial concentration. [Conditions: C_o = 0.5- 800 mg/L (CV), 0.5-600 mg/L (MB) ; pH = 8; Adsorbent dosage = 0.01 g/ 10 ml; T= 298 K].

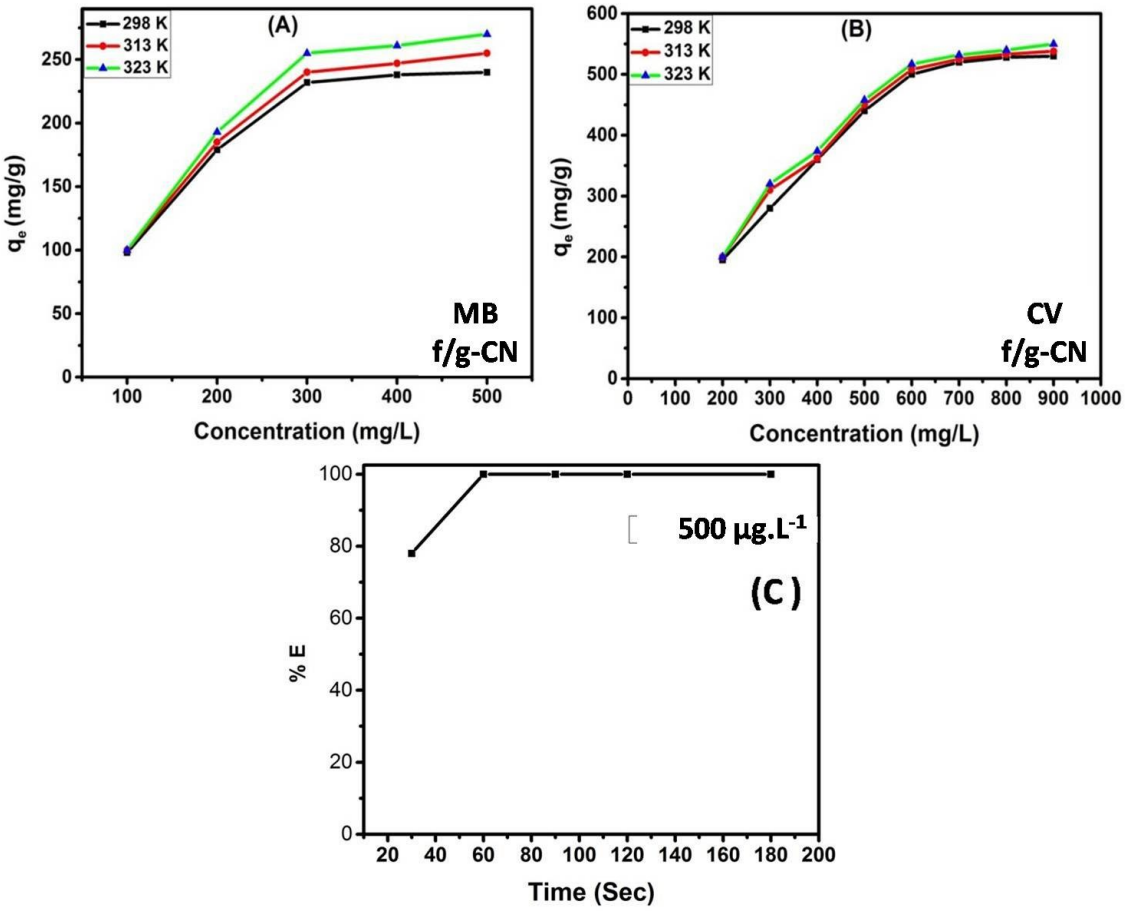

Figure S2: Effect of temperature on MB and CV adsorption onto f/g-CN (A, and B); Effect of contact time on the removal of 500 µg.L^{-1} CV onto f/g-CN (C).

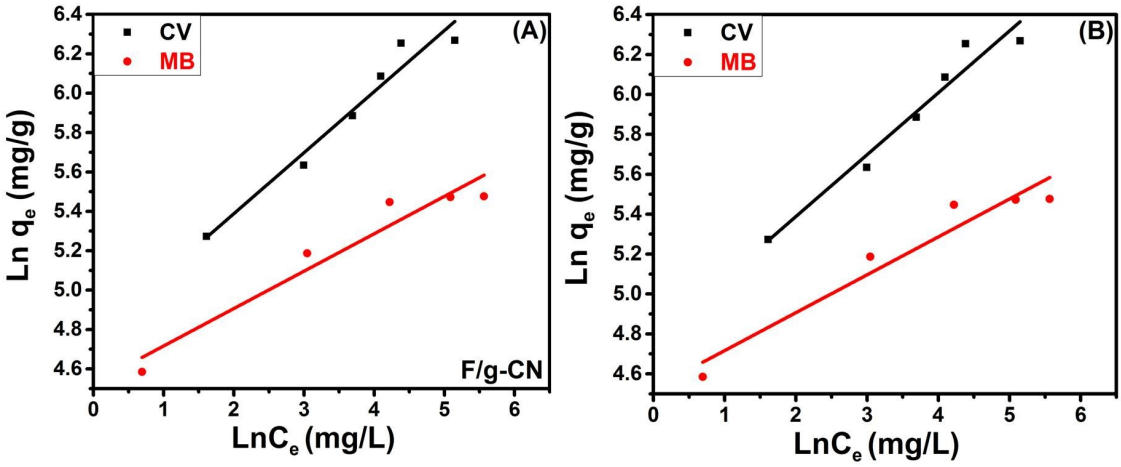

Figure S3: (A) PFO kinetic model and (B) Freundlich adsorption isotherm model.

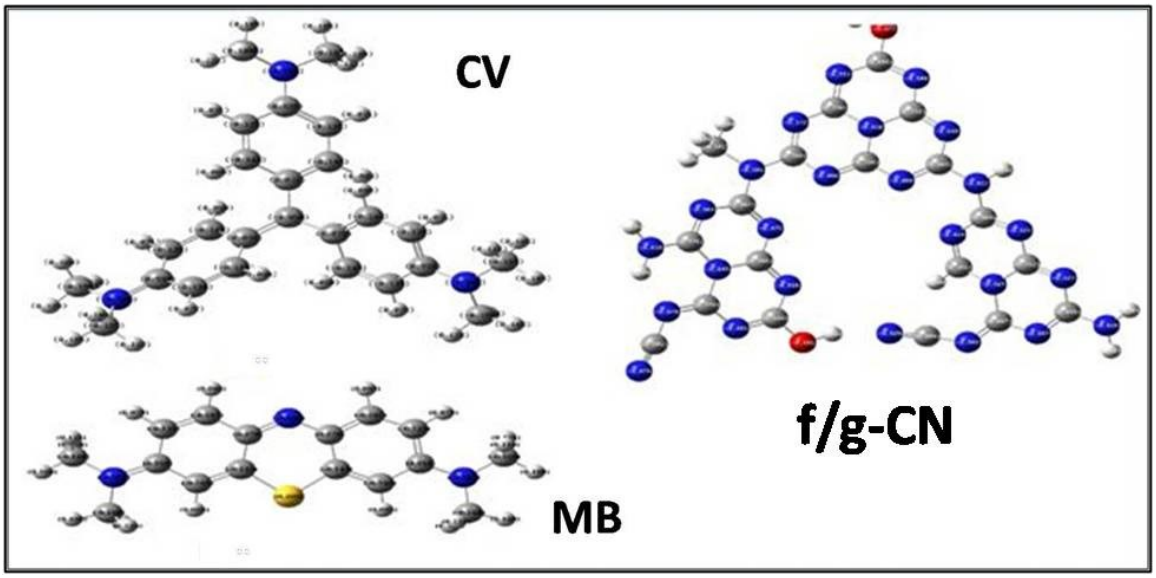

Figure S4: Electron density charge distribution of the MB, CV and f/g-CN**.**

Table S1. The elemental composition of g-CN and f/g-CN from XPS analysis.

Sample	C (%)	O (%)	N (%)
g-CN	45.98	2.62	51.4
f/g-CN	58.23	11.55	30.22

Table S2. The comparison of adsorption capacities of MB and CV through various adsorbents.

Dye	Adsorbent	Adsorption capacity (mg/g)	Reference
MB	NbO/g-C_3N_4	373.1	[6]
	g-C_3N_4/AFP	221.85	[7]
	GO/g-C_3N_4-Fe_3O_4	187.36	[8]
	CMC/PAA/GO	138	[9]
	CMC/Chitosan/GO	122.0	[10]
	C-C_3N_4-20	57.87	[11]
	Chitosan modified zeolite	37.04	[12]
	g-C_3N_4@NiCoLDH	25.16	[13]
	g-CN	28.9	This study
	f/g-CN	239.0	This study
	Biogenic β-CD functionalized	454.5	[14]

CV	Fe° NPs		
	Fe_3O_4 coated biochar	349.4	[15]
	Carboxylate-functionalized cellulose nanocrystals	348.9	[16]
	BAB–AT	280.0	[17]
	Alginate/pectin nanocomposite	251.4	[18]
	Magnetic nanoparticle-modified kaolin	247.7	[19]
	Surfactant modified magnetic nanoadsorbent	166.7	[20]
	Polydopamine/montmorillonite-embedded pullulan hydrogels	112.45	[21]
	AC-Fe_2O_3 NPLs	16.5	[22]
	AA-AMP copolymer adsorbent	9.8	[23]
	g-CN	163.0	This study
	f/g-CN	532.0	This study

Table S3. Electronegativity and electrophilicity of MB, CV, and f/g-CN.

Component	MB	CV	f/g-CN
Electronegativity (χ)	1.874	1.680	4.716
Electrophilicity (ω)	0.981	0.960	7.011

References

1. A. M. El-Wakil, S. M. Waly, W. M. Abou El-Maaty, M. M. Waly, M. Yılmaz and F. S. Awad, ACS omega, 2022, **7**, 6058-6069.
2. F. S. Awad, K. M. AbouZied, W. M. Abou El-Maaty, A. M. El-Wakil and M. S. El-Shall, Arabian Journal of Chemistry, 2020, **13**, 2659-2670.
3. S. Pourbeyram, Industrial & Engineering Chemistry Research, 2016, **55**, 5608-5617.
4. F. A. Pavan, A. C. Mazzocato and Y. Gushikem, Bioresource technology, 2008, **99**, 3162-3165.
5. M. S. Alhumaimess, Separation Science and Technology, 2020, **55**, 1303-1316.
6. Q. Gan, W. Shi, Y. Xing and Y. Hou, Frontiers in chemistry, 2018, **6**, 7.
7. E. G. Sogut, D. Emre, A. Bilici, N. C. Kilic and S. Yilmaz, Materials Chemistry and Physics, 2022, **290**, 126523.
8. S. K. Sahoo, S. Padhiari, S. Biswal, B. Panda and G. Hota, Materials Chemistry and Physics, 2020, **244**, 122710.
9. H. Hosseini, A. Zirakjou, D. J. McClements, V. Goodarzi and W.-H. Chen, Journal of Hazardous Materials, 2022, **421**, 126752.
10. K. Kaur and R. Jindal, Carbohydrate polymers, 2019, **225**, 115245.
11. B. Ren, Y. Xu, L. Zhang and Z. Liu, Journal of the Taiwan Institute of Chemical Engineers, 2018, **88**, 114-120.
12. J. Xie, C. Li, L. Chi and D. Wu, Fuel, 2013, **103**, 480-485.

13. H. Kaur, S. Singh and B. Pal, Korean Journal of Chemical Engineering, 2021, **38**, 1248-1259.
14. J. Nasiri, E. Motamedi, M. R. Naghavi and M. Ghafoori, Journal of Hazardous Materials, 2019, **367**, 325-338.
15. P. Sun, C. Hui, R. Azim Khan, J. Du, Q. Zhang and Y.-H. Zhao, Scientific reports, 2015, **5**, 1-12.
16. H. Qiao, Y. Zhou, F. Yu, E. Wang, Y. Min, Q. Huang, L. Pang and T. Ma, Chemosphere, 2015, **141**, 297-303.
17. J. S. da Silva, M. P. da Rosa, P. H. Beck, E. C. Peres, G. L. Dotto, F. Kessler and F. S. Grasel, Journal of Cleaner Production, 2018, **180**, 386-394.
18. A. Mirza and R. Ahmad, Groundwater for sustainable development, 2020, **11**, 100373.
19. P. Sun, C. Hui, R. A. Khan, X. Guo, S. Yang and Y. Zhao, Journal of Cleaner Production, 2017, **164**, 695-702.
20. C. Muthukumaran, V. M. Sivakumar and M. Thirumarimurugan, Journal of the Taiwan Institute of Chemical Engineers, 2016, **63**, 354-362.
21. X. Qi, Q. Zeng, X. Tong, T. Su, L. Xie, K. Yuan, J. Xu and J. Shen, Journal of Hazardous Materials, 2021, **402**, 123359.
22. S. Hamidzadeh, M. Torabbeigi and S. J. Shahtaheri, Journal of Environmental Health Science and Engineering, 2015, **13**, 1-7.
23. B. Saini and A. Dey, Materials Today: Proceedings, 2022, **61**, 342-350.